

Biliverdin during *Xenopus laevis* Oogenesis and Early Embryogenesis[†]

Marcelo Montorzi,[‡] T. Scott Dziedzic,[‡] and Kenneth H. Falchuk^{*,‡,§,||}

Center for Biochemical and Biophysical Sciences and Medicine and Laboratory for Membrane Transport, Harvard Medical School, One Kendall Square, Building 600, Third Floor, Cambridge, Massachusetts 02139, and Department of Medicine, Brigham and Women's Hospital, 75 Francis Street, Boston, Massachusetts 02115

Received March 13, 2002; Revised Manuscript Received May 30, 2002

ABSTRACT: Biliverdin is required for *Xenopus laevis* embryo dorsal axis formation. When the tetrapyrrole is inactivated by phototransforming it with ultraviolet light prior to the first division, the embryo fails to synthesize dorsal mRNAs, such as *goosecoid* or *chordin*, yet forms increased amounts of ventral transcripts, such as *Vent 1*, and, consequently, develops ventralized morphology. Here we describe the metabolism of biliverdin during oogenesis and early embryogenesis. Estrogen induces frog hepatocytes to synthesize biliverdin and vitellogenin. The two molecules form a complex that is secreted into and transported in the plasma to be taken up by the oocyte as it matures through its six stages of oogenesis. In the oocyte, the biliverdin–vitellogenin complex is processed and stored in the yolk platelets. In these organelles, biliverdin is associated entirely with the lipovitellin domain of the processed vitellogenin. Once the egg is fertilized, its biliverdin content decreases over a 5–6 h period to participate in the chemical machinery required for dorsal axis formation. This participation must be initiated during the period encompassing the first embryonic mitosis. The results describe the pathway that generates, transports, and stores biliverdin as part of oogenesis, define the time course for its utilization after fertilization, and link biliverdin to the metabolism of the phosphoglycolipometalloprotein, vitellogenin.

Embryo morphogenesis requires establishment of both molecular and structural asymmetries between the dorsal and ventral zones within the first few cell divisions after fertilization (1). The dorsal zone then generates mRNAs responsible for head structures, spinal cord, and other dorsal organs. Failure to form these transcripts leads to predominance of the ventral zone mRNAs that result in embryo ventralization characterized by the absence of these dorsal organs (2, 4). The entire process is mediated largely by diverse chemical signals (3, 4). We reported that one of those signals is the tetrapyrrole biliverdin. It plays a hitherto unrecognized and essential role in the earliest stages of embryogenesis to mandate dorsal axis formation (2). This essentiality of biliverdin has been ascertained by virtue of its sensitivity to in vivo UV light irradiation of the vegetal hemisphere of the embryo and the consequences that follow that exposure. Thus, when the stage 1 embryo is exposed to either short (254 nm) or long (366 nm) UV light prior to the first cleavage, its biliverdin is phototransformed. The result is that downstream dorsal mRNA markers, e.g., *goosecoid* and *chordin*, are not expressed while that of the ventral mRNA marker, *Vent 1*, is up-regulated (2, 5). The irradiated, biliverdin-depleted embryos develop significant axis deficiency, quantified by a reduction in the dorsal anterior index

(DAI) from a normal of 5 to less than 2, with many having complete absence of any dorsal axis scored with a DAI of 0. Remarkably, if the irradiated embryos are incubated with intact biliverdin after termination of UV-irradiation, the embryos recover their capacity to develop a dorsal axis; over 60–70% are fully rescued and generate embryos with a normal DAI of 4–5 (2).

The identification of this mandatory function for biliverdin in dorsal axis formation calls for examination of its metabolism in both maternal and embryo tissues, the structural requirements for its function, and definition of any molecular partners with which may it interact. A starting conceptual point for this undertaking derives from the understanding that other molecules required for developmental and differentiation processes—metals, retinoids, prostaglandins—are transported from, into, and within cells through binding to one or more proteins to exert their biological actions (6, 7). Here we demonstrate that biliverdin metabolism is linked to and depends on a major protein that both transports it into and stores it in the oocyte. We also identify the timing of its release from the storage site and utilization following fertilization. The stage is set to identify yet additional protein partners essential for subsequent development.

EXPERIMENTAL PROCEDURES

The time course for appearance and accumulation of biliverdin in oocytes during oogenesis, its distribution within intraoocyte compartments, and its utilization during early embryogenesis were examined by using oocytes at different stages of maturation, selected according to standard morphological criteria (8). Early stage (I and II) oocytes were obtained directly from the ovaries of 2–3 cm length young

[†] This work was supported by the Endowment for Research in Human Biology, Inc., and by Brigham and Women's Hospital Research Fund Grant 645912.

* To whom correspondence should be addressed. Telephone: (617) 621-6126. E-mail: kenneth_falchuk@hms.harvard.edu.

[‡] Center for Biochemical and Biophysical Sciences and Medicine, Harvard Medical School.

[§] Department of Medicine, Brigham and Women's Hospital.

^{||} Laboratory for Membrane Transport, Harvard Medical School.

female frogs. Stages III–VI oocytes were obtained by dissection of adult 6–7 cm frog ovaries as previously described (9). Both pigmented and albino adult *Xenopus laevis* female frogs (6–7 cm) were used to obtain spawned eggs. The presence of biliverdin and its distribution within the egg intracellular compartment was determined using 200 freshly spawned dejellied eggs from both types of frogs. The eggs were manually homogenized in 5 volumes of 0.25 M sucrose, 20 mM Tris, 50 μ M leupeptin, pH 7.5, 2 °C (buffer A). One milliliter of the homogenate was loaded onto a 5 mL stepwise sucrose gradient and spun in an SW40 rotor (Beckman) at 25 000 rpm, 0 °C, for 22 h as described previously (8, 9). Five egg fractions were separated by the following density step-gradient (in g/mL): <1.07, 1.08, 1.15, 1.16, 1.20, 1.21, 1.26, 1.27, and 1.30. One volume of the sample was mixed with 2 volumes of organic extraction solvent (8 parts ethyl acetate, 1 part methyl acetate, and 50 μ g/mL butylated hydroxytoluene) (2) to extract the biliverdin from each gradient fraction. The fraction of the biphasic immiscible mix that retained the green color characteristic of biliverdin was recovered and dried.

The dried nonvolatile residuals obtained from each extract were dissolved in 10% acetonitrile, 10 mM ammonium acetate, pH 6.5. Aliquots of 250 μ L were loaded onto a Jupiter 5 μ C₁₈ 300 Å 250 × 4.6 mm column (Phenomenex) connected to a Waters 510 HPLC pump and a Waters Automated Gradient Controller and eluted with a binary solvent system. The initial solvent was ammonium acetate 10 mM, pH 6.5, and the final buffer was 100% acetonitrile. The gradient design was: 0–100% ending solvent with a linear increment from 5 to 45 min, then 100% ending solvent from 45 to 60 min. The eluate was monitored at 340 nm with a Waters 440 Absorbance Detector, and the data were recorded with a Hewlett-Packard 3390 Integrator. The retention times for the known chemicals biliverdin IX α , *all-trans*-retinoic acid, 9-*cis*-retinoic acid, and α -carotene were determined with commercially available compounds (Sigma, St. Louis, MO). Each sample was treated similarly with organic solvents, chromatographed under the same conditions. The results were used to study the presence and content of these molecules in the different fractions prepared for analysis. A wavelength absorbance scan was performed on selected fractions with a Varian-Cary 50 Bio UV–Vis spectrophotometer. Selected HPLC samples were dissolved in equal volumes with methanol and submitted to mass spectrometric analysis with a Finnigan LCQ ion trap mass spectrometer.

Spawned eggs were fertilized *in vitro*, and the embryos were staged according to the standard *X. laevis* developmental table (10, 11). The time frame following fertilization during which biliverdin must be inactivated by UV light to prevent dorsal axis formation has been reported (2). Oocytes and embryos selected at targeted stages of development were homogenized in 1 volume of ice-cold stabilizing buffer composed of EDTA¹ 30 mM, ascorbic acid 30 mM, Tris 20 mM, pH 7.4. Oocyte and embryo homogenates were extracted, and their biliverdin content was analyzed as described above.

Vitellogenin was purified from the serum of adult female *X. laevis* frogs according to previously reported methods (12). The animals were injected in the dorsal lymph sac with 2 mg of estradiol valerate (Bristol-Myers-Squibb Co., NJ). Twenty-one days later, the frogs were anesthetized, and their blood was extracted by direct heart puncture. The serum was diluted 1:1 with Tris 20 mM, pH 7.5. One milliliter of the sample was chromatographed in an HR 5/5 column packed with 1 cm³ of Source 15Q resin (Amersham-Pharmacia Biotech, NJ) using an FPLC system (Pharmacia) at a flow rate of 2 mL/min. Initial buffer was Tris 20 mM, pH 7.5, and final buffer was NaCl 1 M, Tris 20 mM, pH 7.5. The gradient design was 0–50% final buffer with a linear increment from 5 to 20 min. The eluate was recorded at 284 nm. The absorption at 375 nm was determined in the collected fractions with a Varian-Cary 50 Bio UV–Vis spectrophotometer. The fractions with absorbance at 375 nm higher than twice the background signal were extracted with organic solvents using a ternary system consisting of 1 part of chloroform and 2 parts of methanol added to 0.8 part of either the serum or the selected fractions (13). This solvent mixture differs from the one used with the oocyte constituents (see above) because the latter was ineffective in extracting the blue–green pigment from serum fractions.

The yolk platelet proteins were purified from solubilized organelles (12, 14). Yolk platelets were dissolved in 2 volumes of NaCl 1.5 M, Tris 30 mM, pH 7.5, 2 °C (buffer B). The solubilized proteins from the yolk platelets were separated by selective precipitation with ammonium sulfate to a final concentration of 66% of the saturated concentration. The resultant ammonium sulfate suspension was spun at 30 000 rpm in a Beckman Ti80 rotor for 60 min at 2 °C. The supernatant contains phosvitin while the pellet is composed principally of lipovitellin. The latter was redissolved in buffer B and reprecipitated with ammonium sulfate as described above. Finally, lipovitellin was dissolved in 2 volumes of buffer B. One milliliter of the lipovitellin solution was loaded onto a 120 × 1 cm glass column (Bio-Rad) packed with Sephacryl S-300 resin (Pharmacia), previously equilibrated with 1 M NaCl, 30 mM Tris, pH 7.5 (buffer C), at room temperature. The flow rate was 4.5 mL/h, and fractions of 2 mL each were collected. Fractions were individually read for their absorption at 280 and 375 nm with a Varian-Cary 50 Bio UV–Vis spectrophotometer. Standard SDS–polyacrylamide gel electrophoresis and amino acid analyses were performed as described (12).

The fractions with high absorbance at 375 nm were extracted with the same ethyl acetate/methyl acetate mixture as used with the oocyte and embryo homogenates. The resultant extracts were chromatographed by reversed phase HPLC as described (2). The HPLC fractions eluting at 23.3 min from either the lipovitellin or the vitellogenin extracts were analyzed by mass and UV–Vis spectrometry and compared with the spectrum of a commercial biliverdin standard sample that was treated previously in a similar way, by organic solvents and HPLC separation.

RESULTS

The methyl acetate/ethyl acetate solvent mixture extracts the blue–green pigment biliverdin from all frog eggs (2). In addition, a number of other compounds are also extracted.

¹ Abbreviations: EDTA, ethylenediaminetetraacetic acid; VG, vitellogenin; LV1, lipovitellin 1; LV2, lipovitellin 2; PV, phosvitin; *T*_{fm}, time from fertilization in hours.

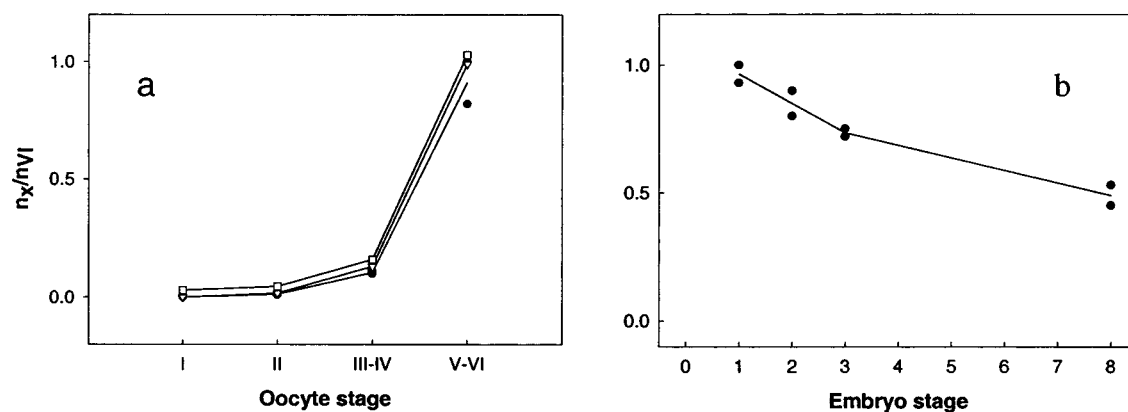


FIGURE 1: Changes in biliverdin content during oogenesis and early embryogenesis. (a) Normalized values for oocyte volume and their biliverdin and zinc contents at different stages of maturation. The ratios represent the value of the measured variable at any given stage (n_x) divided by the value at stage VI (n_{vi}). Zinc and volume values for each oocyte maturation stage were adapted from previous publications (1, 9). The content of biliverdin was performed in duplicate batches of 300–600 eggs or embryos. The biliverdin content increases progressively during oogenesis (●). Its incremental accumulation correlates with that of zinc (□) and volume (▽). (b) In the embryo, the biliverdin content (●) decreases steadily after fertilization. At stage 8, it has decreased to less than half of the original amount in the egg.

All of them have distinct hydrophobic properties that define different elution times from a C18 HPLC column. Biliverdin is one of the least hydrophobic constituents and elutes at 23.3 min with 44% acetonitrile. Other more hydrophobic compounds elute with higher amounts of acetonitrile. Two of these compounds elute with retention times that are identical to the *all-trans*-retinoic acid and α -carotene standards. These differences in elution times allowed us to separate these compounds, quantitate their presence, and determine the time course of their accumulation in oocytes. For example, α -carotene is already present in stage I oocytes, and its peak area varies minimally during oogenesis (not shown). In contrast, the peak corresponding to biliverdin is barely detectable in stage I–II oocytes, but its peak area increases significantly and progressively in stages III–VI (Figure 1), known as the vitellogenic phase. The increase in biliverdin content is concurrent with major morphological changes of the oocyte. The color of oocytes from pigmented frogs is altered as they progress through oogenesis. They are white in stage I, pale brown in stage II, and progressively greener as they develop from stage III to stage IV.

The relative changes in egg biliverdin content during the vitellogenic phase are identical to those observed for zinc (9, 12, 14) and volume increase (1, 15, 16). Thus, the curves describing the incremental accumulation of zinc and the increase in volume during oogenesis correlate closely with that of biliverdin (Figure 1). We had previously demonstrated that zinc incorporation by the oocyte depends on the import of zinc-vitellogenin and subsequent processing into the yolk platelet proteins zinc-lipovitellin and phosvitin. Thus, vitellogenin contains 1 mol of zinc per monomer (12), and this zinc in vitellogenin accounts for well over 95% of the zinc in the oocyte (14). Hence, any increase in zinc corresponds to an increase in vitellogenin. As greater quantities of vitellogenin are taken in and processed within yolk platelets, these organelles increase both in size and in density, leading to an increase in oocyte volume (16). Therefore, since the time course of biliverdin accumulation during oogenesis correlates to these other two variables, it is consistent with the conclusion that the tetrapyrrole is a yolk platelet constituent and that its accumulation in the oocyte also is governed by the processes associated with yolk formation.

Table 1: Distribution of Biliverdin in Subcellular Fractions of *Xenopus laevis* Eggs

fraction δ (g/mL)	typical components	peak area ^a	peak area ^a (% of total)
<1.07	lipids	0	0
1.08–1.15	cytosol	0	0
1.16–1.20	mitochondria	0	0
1.21–1.26	yolk platelets	36.87	73.8
1.27–1.30	peroxisomes, nuclei	9.66	26.2

^a Peak area of the biliverdin fraction present in the HPLC chromatogram recorded at 340 nm.

This premise is now confirmed. Isopycnic fractionation of egg homogenates separates cytosol, mitochondria, light and dense yolk platelets, nuclei, and peroxisomes (12). Analysis of the biliverdin content in these egg constituents demonstrates that the tetrapyrrole is found predominantly in fractions with densities between 1.21 and 1.23 g/mL, layers that concentrate and separate yolk platelets (Table 1). Therefore, the majority of egg biliverdin is localized to yolk platelets. A smaller amount of biliverdin appears in the heavier fractions that typically contain peroxisomes and nuclei, but may also contain the heaviest and densest yolk platelets or represent a carry-over phenomenon of yolk platelets as the fractions are collected. No biliverdin is found in any other layer.

Its presence in yolk platelets is explained by the observation that biliverdin is an intrinsic component of vitellogenin. After estrogen administration, vitellogenin synthesis is induced in the frog's liver and secreted into the bloodstream. The normally yellow plasma acquires an intense green color. This change in color is due entirely to the presence of biliverdin. The organic solvent extract of the blue–green serum chromatographed on a C₁₈ column demonstrates that the blue–green fraction elutes with a retention time of 23.3 min (Figure 2a). This peak fraction exhibits a characteristic UV–Vis absorption profile with two distinctive peaks at 375 and 665 nm (Figure 2b). Its mass is (+1) 583.25 *m/z* (Figure 2c). These physical chemical characteristics identify the blue–green fraction as biliverdin (2).

The biliverdin in serum is bound to vitellogenin. Protein components of the blue–green serum are chromatographed

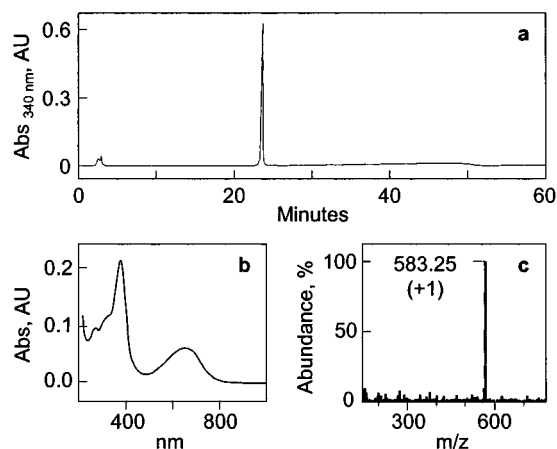


FIGURE 2: Physical-chemical properties of the blue-green pigment from serum of estrogen-stimulated frogs. (a) Rechromatography of an HPLC-purified blue-green fraction from serum yields a sharp peak that elutes at 23.3 min. (b) UV-Vis spectrometric analysis of this fraction reveals characteristic absorption peaks at 375 and 665 nm. (c) Mass spectrometric analysis of this fraction indicates that it has a mass identical to that of a biliverdin standard.

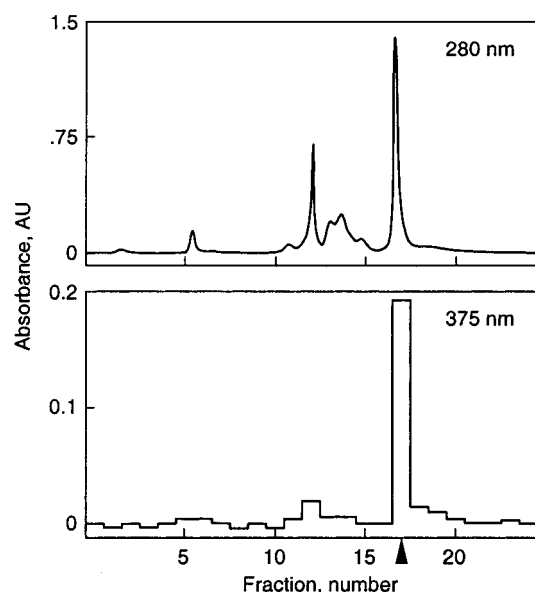


FIGURE 3: Vitellogenin purification from frog serum by Fast Protein Liquid Chromatography. A source 15Q resin was used for the chromatography of the serum. (a) The serum contains a number of proteins that are resolved into distinctive peaks monitored at 280 nm. (b) Only one fraction (arrowhead) retains the blue-green color of the serum. The chromophore is identified as biliverdin by the identical criteria shown in Figure 1.

with a Source 15Q resin. Many of the eluting fractions absorb at 280 nm, but only fractions 17 and 18 also absorb significantly at 375 nm (Figure 3). Furthermore, these fractions are the only ones that retain the blue-green color of the serum loaded onto the column. The amino acid composition of peak fraction 17 (Figure 4) is comparable to literature values for vitellogenin (12) and confirms that fractions 17 and 18 contain pure vitellogenin. The blue-green chromophore, extracted separately with organic solvents from purified vitellogenin, has a retention time and spectral characteristics identical to those of biliverdin extracted directly from serum (Figure 2). Therefore, the presence of a biliverdin-vitellogenin complex in the serum of estrogen-stimulated frogs determines its green color.

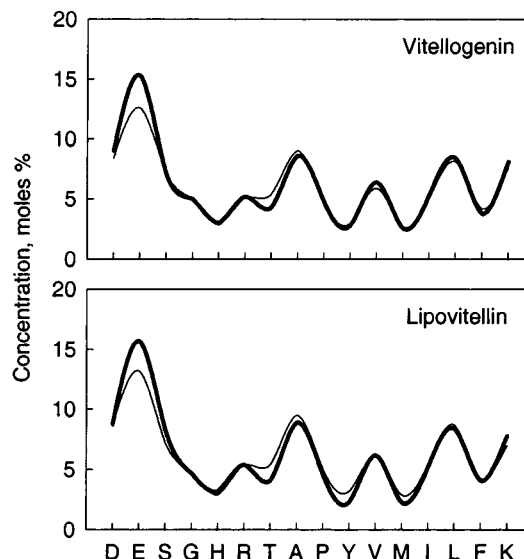


FIGURE 4: Amino acid analysis. The abundance of each amino acid analyzed was calculated and plotted in percent of the total moles measured. The present values (heavy lines) were compared to reference ones (light lines) of either vitellogenin or lipovitellin (12). (a) Comparison of fraction 17 (see Figure 3) with vitellogenin reference. (b) Comparison of fraction 15 (see Figure 5) with lipovitellin reference.

Biliverdin is associated with lipovitellin in the yolk platelets. The yolk platelet proteins are solubilized with NaCl. Lipovitellin can be separated from phosvitin by treatment with ammonium sulfate because the former is selectively precipitated while the latter remains in the supernatant after ultracentrifugation. The pellet containing lipovitellin is blue-green and exhibits absorption peaks at 375 and 665 nm characteristic of biliverdin. The phosvitin-containing ammonium sulfate supernatant is not blue-green and, therefore, does not absorb at the higher wavelength. Size exclusion chromatography on a Sephacryl S-300 column further purifies lipovitellin by separating smaller peptide fragments from the LV1-LV2 complex (Figure 5). Fractions 14-18 collected from the size exclusion chromatography experiment absorb both at 280 and at 375 nm. Peak fraction 15 resolves into three bands on SDS gel electrophoresis (Figure 5 inset). The bands are identified with Coomassie blue staining. The larger one displays an electrophoretic migration close to the 115 kDa marker, and the two smaller ones migrate close to the 34.8 kDa marker. These values, in conjunction with the morphology of the bands, are consistent with the reported molecular masses of lipovitellin 1 (~115 kDa), lipovitellin 2 α (~35 kDa), and lipovitellin 2 β (~32 kDa) (12, 17, 18). The amino acid composition of fraction 15 confirms the assignment of the identity of the protein as lipovitellin and certifies the peak as pure (Figure 4). The amino acid content (mole percent) is comparable to the reference amino acid composition of lipovitellin (12). Therefore, the peaks recorded at 280 and 375 nm coelute in the same fractions and contain lipovitellin 1 and lipovitellin 2 in complex form.

The blue-green chromophore of lipovitellin was extracted with organic solvents, and the extracted material was resolved by HPLC on a C₁₈ column. The HPLC elution profile of the lipovitellin extract recorded at 340 nm reveals one main peak with a retention time of 23.3 min, identical to the retention time of the extracts from vitellogenin, the oocytes and eggs (Figure 2a). The UV-Vis absorption spectrum (Figure 2b)

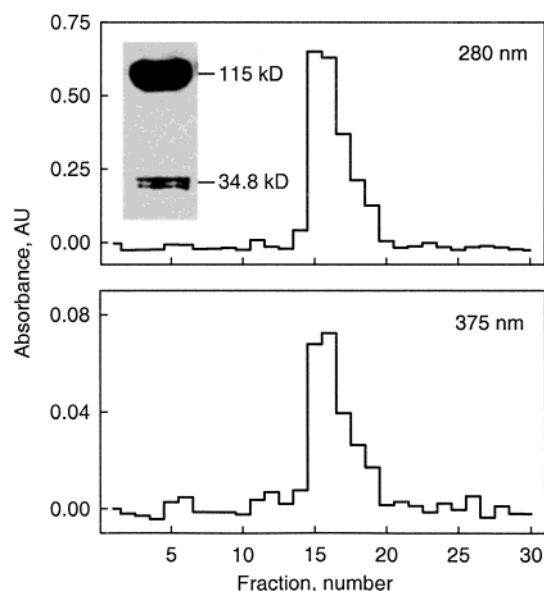


FIGURE 5: Size exclusion Sephacryl S-300 column chromatography of lipovitellin. A single predominant peak (fractions 14–18) absorbs significantly at (a) 280 and (b) 375 nm entirely due to the presence of biliverdin. Inset: SDS–polyacrylamide gel electrophoresis of fraction 15 (peak). Three separate bands are resolved, consistent with LV1, LV2 α , and LV2 β . The marks next to the gel correspond to the relative mobilities of the molecular weight standards.

and molecular mass (Figure 2c) of this fraction are characteristic of biliverdin. Both results also are identical to the characteristics of purified commercial biliverdin used as standard (2). Jointly, these results indicate that biliverdin is bound to lipovitellin in the yolk platelets.

Whereas biliverdin increases progressively during the year-long process of oogenesis (Figure 1), once the egg is fertilized, its content in the embryo decreases within hours. By the time the embryo reaches stage 2 (four cells), it has fallen by 20%, and it falls further to 50% during the next 5–7 h, the period required to reach stage 8 of development (Figure 1).

DISCUSSION

We recently reported that biliverdin IX α is a normal constituent of *Xenopus laevis* oocytes and eggs and has a role in the establishment of the dorsal axis and generation of corresponding organs in embryos (2). The biliverdin in the mature, fertilized egg can be phototransformed when ultraviolet light is applied to the vegetal surface of the embryo prior to the first division. The developmental outcomes of the phototransformation are ventralized embryos that fail to form dorsal organs such as brain, eyes, spinal cord, etc. Replenishing biliverdin prior to the end of the second division reestablishes the lost capability to form dorsal organs. These novel findings shift our understanding of the biological significance of this tetrapyrrole from that of a breakdown product of heme without a functional purpose to that of a molecule essential for embryogenesis. It calls for placing it as a component of the current framework of signaling molecules and their activators, inhibitors, and/or regulators of posttranslational metabolism involved with formation of dorsal organs. These conclusions compelled us to extend our studies with this tetrapyrrole and delineate its metabolism during *X. laevis* oogenesis and early embry-

genesis. We find that the elements of that metabolism are intimately linked to that of the major egg protein vitellogenin, its processed product lipovitellin, and its storage organelle. Those aspects of biliverdin metabolism that pertain to the period of oogenesis include hormonal regulation of its synthesis, association with vitellogenin as a carrier protein synthesized in the liver, secretion into plasma, and transportation into and storage in the oocyte (Figures 1–6, Table 1). Those that relate to the post-fertilization period depict biliverdin release from storage following fertilization during the early stages of embryogenesis (Figure 1).

Thus, biliverdin IX α has been shown to be an intrinsic constituent of vitellogenin (Figures 3 and 4). This 220 kDa protein is already known to be of major importance to embryo development since it serves as the carrier of several elements essential for embryogenesis including phosphate, carbohydrate, lipid, zinc, and calcium. The association of yet another essential molecule with vitellogenin, therefore, is consistent with this function. Biliverdin, like all of the other intrinsic constituents of vitellogenin, must be incorporated during its estrogen-activated synthesis in the hepatocyte since the protein contains all of these molecules that it transports by the time it is secreted into the plasma (12, 19–21). This requires that sufficient amounts of biliverdin be available to associate with nascent vitellogenin and leads to the conclusion that estrogen administration, either directly or indirectly, must up-regulate the formation of the tetrapyrrole itself. A point of departure to begin to understand how the tetrapyrrole might be formed and how its metabolism might be linked to that of vitellogenin is to review the available information on biliverdin biochemistry in juxtaposition with vitellogenin synthesis in the liver and its processing in the oocyte (Figure 6). Biliverdin is formed by the action of the microsomal enzyme heme-oxygenase (HO-1) that catalyzes the oxidation of heme to α -OH-hemin with a ferric (Fe^{3+}) cation (22, 23). Then, in a subsequent nonenzymatic step, biliverdin is generated after the release of Fe^{3+} and a molecule of carbon monoxide (24). While the above biochemical scheme relates to heme breakdown, analogous enzymatic machinery may also be operative in the frog. In this case, however, the enzymatic activity needs to be understood as part of a primary synthetic rather than a degradation process.

Once the biliverdin–vitellogenin complex is formed, the protein acts as the vehicle to transport biliverdin in the plasma from its hepatic site of origin to its storage site in the oocyte. Normally, the frog's plasma is yellow, but following a high-dose estrogen administration, it becomes blue–green owing to the high amount of biliverdin–vitellogenin product induced by the hormonal stimulation and secretion into the bloodstream (Figure 2). The estrogen effects on biliverdin/vitellogenin synthesis in female frogs have been reproduced in male frogs whose plasma normally does not contain vitellogenin (12).

Biliverdin is brought into the oocyte when the biliverdin–vitellogenin complex in the plasma is internalized after binding to oocyte membrane receptors on coated pits (25). Once in the oocyte, the biliverdin–vitellogenin complex is processed within endocytosed vesicles that fuse with multivesicular bodies and then to yolk platelets. In these organelles, vitellogenin is hydrolyzed into various fragments that comprise lipovitellin 1 (LV1, ~115 kDa), lipovitellin 2

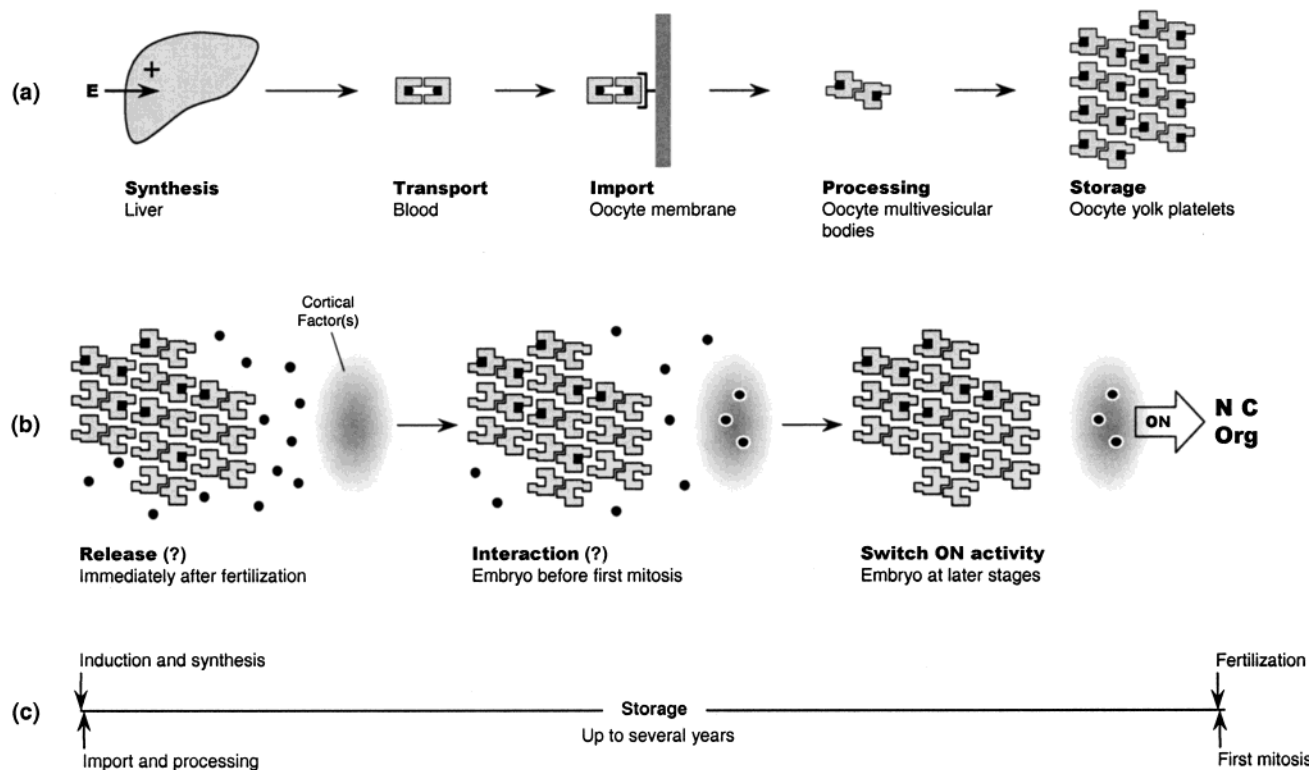


FIGURE 6: Proposed model of the metabolic pathway of *X. laevis* biliverdin. (a) Estrogen (E) induces hepatocytes to synthesize vitellogenin and biliverdin (●). The biliverdin–vitellogenin complex is excreted into the frog plasma and binds to oocyte receptors, and it is internalized. The complex is processed into lipovitellin/phosvitin domains. Lipovitellin contains the biliverdin. (b) After fertilization, biliverdin is proposed to be released to interact with a cortical factor(s) as a mandatory step to switch ON and establish the dorsalizing centers, the Nieuwkoop center (NC), and the Spemann–Mangold organizer (Org). (c) Time line for biliverdin production, storage, and activity.

(LV2 α , ~35 kDa; LV2 β , ~32 kDa) and phosvitin (PV, ~39 kDa). The resulting protein fragments (LV1, LV2, and PV) remain together in the form of a complex that polymerizes in a quite characteristic microcrystalline array that has been resolved by electron microscopy (26, 27). The biliverdin is located in the vitellogenin domain that is processed into lipovitellin in the yolk platelet (Figures 4 and 5, Table 1). The lipovitellin–tetrapyrrole complexes are stored in these organelles for several years, the period of time that it takes for an oocyte to develop from stage I to stage VI (1, 28). These findings provide unambiguous proof of a previously proposed association of biliverdin with lipovitellin (29, 30).

Treatment with ethyl acetate/methyl acetate easily extracts the biliverdin from lipovitellin whether as found within oocytes, within yolk platelets, or as the purified protein, suggesting biliverdin binding is likely noncovalent. In contrast, different conditions are required to extract the tetrapyrrole from vitellogenin. Thus, the organic solvent extraction protocol used to extract biliverdin from lipovitellin fails to extract the pigment from the parent vitellogenin. An alternative ternary system (chloroform, methanol, and the aqueous sample) was required to extract biliverdin from vitellogenin either as the pure molecule or as found in serum. The basis for this difference in extractability needs to be evaluated. It indicates the presence of distinct chemical environments in the parent and its processed product that may impact on the exposure of the biliverdin-carrying site to the surrounding solvent.

Once the egg is fertilized, the biliverdin must be asymmetrically distributed since during this early period the

tetrapyrrole concentrates in the vegetal hemisphere as the majority of the yolk platelets settle into that pole of the embryo (1). The significance to the embryo is that during these first hours the content of biliverdin decreases by 50% in the region that contains the determinants of future dorsal organs (Figure 1b). The identities and functions of many of the molecules that comprise the cortical determinant(s) and participate in this complex embryological process have been studied and organized into two signaling pathways: the canonical Wnt/ β catenin and nonclassical one consisting of, e.g., TGF β -like factors that enhance the dorsalizing capabilities of the classical pathway (2–5, 31–33).

We proposed that biliverdin is released during the narrow window of time before the first mitosis to bind one or more cortical determinants to participate in the series of events that result in the formation of the dorsal axis in the embryo and induce dorsal structures (2). It is now necessary to examine how, where, and with what components of the classical system does biliverdin interact and how it fits in the framework of these signaling pathways. β catenin is a central participant of both pathways. It is present in the cortex of both animal and vegetal poles of the egg (34, 35) and is redistributed to the dorsal zone after fertilization within one to two cell divisions. There it is relocated from the cortex to the cytoplasm. Once in the cytoplasm, it binds to a group of proteins that lead either to its stabilization and translocation into the nucleus or to its degradation by ubiquitin-dependent proteolysis. The selection of the fate depends, in part, on the amounts and functionalities of a complex of proteins associated directly or indirectly with β catenin (32). When

the predominant complex is with the phosphorylating enzyme glycogen synthase 3 (GSK3 β), CK1 α , APC, axin, and others, then β catenin is phosphorylated and subsequently degraded. When the predominant complex is with the products of activation initiated by Wnt ligand-binding to Frizzled receptors, including Dishevelled, β catenin is stabilized (32, 33, 36). Stable cytoplasmic β catenin is translocated to the nuclei of cells in the dorso-vegetal zone. The nuclear localization is associated with binding to HMG box transcription factor Tcf and activation of transcription of siamois followed by a host of other target genes (37–39).

There are tantalizing results that point to the participation of biliverdin in this classical system. Thus, biliverdin acts early in embryogenesis since its must be inactivated prior to the first cell division in order to result in failure to establish dorsal structures. Moreover, recovery of the lost capability of UV-irradiated embryos is only possible if biliverdin is replenished no later than the period between the end of the first and the beginning of the second division (2). This is the same time frame when the canonical signaling system initiates its actions to produce dorsal axis, specifically activation of Wnt signals, translation, and redistribution of β catenin to the dorsoequatorial region. It is also the period when UV irradiation both transforms biliverdin (2) and concurrently increases the content in the dorsal zone of GSK3 β , the protein that phosphorylates β catenin and results in its degradation (40). Similarly, UV irradiation both transforms biliverdin and causes failure to form dorsal mRNA markers mediated by β catenin gene activation (2). Thus, biliverdin could affect the quantity, stability, and/or activity of β catenin, GSK3 β , or any other of the molecules involved in the signaling pathway. Studies are in progress to examine these molecules in embryos with intact biliverdin, biliverdin depleted (UV irradiated), and biliverdin repleted (UV irradiated incubated with biliverdin).

The findings that biliverdin binds normally to the highly conserved vitellogenin and lipovitellin, proteins of recognized importance to development, together with the prolonged effort expended by the frog to accumulate and store the tetrapyrrole in yolk platelets and the effects of ultraviolet light on development provide further support for the view that the molecule has a significant function in biology. Similar conclusions can be made for both vitellogenin and lipovitellin, long considered to constitute a maternal–oocyte nutrient transport and storage system for metals, amino acids, hydrocarbons, phosphates, and lipids that supply the developing embryo with these essential compounds (12, 17, 18, 41). In the context of the essential role of biliverdin in frog embryogenesis, its addition to the molecules associated with vitellogenin and lipovitellin broadens the importance of these proteins. Vitellogenin now must be recognized to function as a major transport, protective shield, delivery, and storage system for biliverdin. It is now necessary to define the molecular partners that interact with biliverdin following its proposed release from the yolk platelet during the first cell divisions of the embryo and affect downstream transcription of both dorsal and ventral mRNAs (Figure 6).

ACKNOWLEDGMENT

We are grateful to Drs. James Riordan and Bert L. Vallee for their valuable advice and suggestions in the preparation of the manuscript.

REFERENCES

- Hausen, P., and Riebesell, M. (1991) in *The early development of Xenopus laevis*, pp 1–25, Springer-Verlag, New York.
- Falchuk, K. H., Contin, J. M., Dziedzic, T. S., French, T. C., Feng, Z., Heffron, G. J., and Montorzi, M. (2002) A role for biliverdin IX α in dorsal axis development of *Xenopus laevis* embryos. *Proc. Natl. Acad. Sci. U.S.A.* 99, 252–256.
- Heasman, J. (1997) Patterning the *Xenopus* blastula. *Development* 124, 4179–4191.
- Nieto, M. A. (1999) Reorganizing the organizer 75 years on. *Cell* 98, 536–545.
- Steinbeisser, H., De Robertis, E. M., Ku, M., Kessler, D. S., and Melton, D. A. (1993) Induction of *gooseoid* injected *wnt-8* and *activin* mRNA. *Development* 118, 499–507.
- Vallee, B. L., and Falchuk, K. H. (1993) The biochemical basis of zinc physiology. *Physiol. Rev.* 73, 79–118.
- Lohnes, D., Dierich, A., Ghyselinc, K., Kastner, P., Kanron, C., Le Meur, M., Lufkin, T., Mendelsohn, C., Naskhartri, H., and Chambon, P. (1992) Retinoid reception and binding proteins. *J. Cell Sci. Suppl.* 16, 69–76.
- Dumont, J. N. (1972) Oogenesis in *Xenopus laevis* (Daudin). Stages of oocyte development in laboratory maintained animals. *J. Morphol.* 136, 153–179.
- Nomizu, T., Falchuk, K. H., and Vallee, B. L. (1993) Zinc, iron and copper content of *X. laevis* oocytes and embryos. *Mol. Reprod. Dev.* 36, 419–423.
- Nieuwkoop, P. D., and Faber J. (1967) *Normal table of Xenopus laevis* (Daudin), 2nd ed., North-Holland Publishing Co., Amsterdam.
- Kao, K. R., and Ellinson, R. P. (1988) The entire mesodermal mantle behaves as Spemann's organizer in dorsoanterior enhanced *Xenopus laevis* embryos. *Dev. Biol.* 127, 64–77.
- Montorzi, M., Falchuk, K. H., and Vallee, B. L. (1995) Vitellogenin and lipovitellin: zinc proteins of *X. laevis* oocytes. *Biochemistry* 34, 10851–10858.
- Bligh, E. G., and Dyer, W. J. (1959) A rapid method of total lipid extraction and purification. *Can. J. Biochem. Physiol.* 37, 911–917.
- Falchuk, K. H., Montorzi, M., and Vallee, B. L. (1995) Zinc uptake and distribution in *X. laevis* oocytes and embryos. *Biochemistry* 34, 16524–16531.
- Wall, D. A., and Patel, S. (1987) The intracellular fate of vitellogenin in *Xenopus* oocytes is determined by its extracellular concentration during endocytosis. *J. Biol. Chem.* 262, 14779–14789.
- Danilchik, M. V., and Gerhart, J. C. (1987) Differentiation of the animal–vegetal axis in *Xenopus laevis* oocytes. I. Polarized intracellular translocation of platelets establishes the yolk gradient. *Dev. Biol.* 122, 101–112.
- Ohlendorf, D., Barbarash, G., Trout, A., Kent, C., and Banaszak, L. (1977) Lipid and polypeptide components of the crystalline yolk system from *Xenopus laevis*. *J. Biol. Chem.* 252, 7992–8001.
- Wiley, H. S., and Wallace, R. A. (1981) The structure of vitellogenin. Multiple vitellogenins in *Xenopus laevis* give rise to multiple forms of the yolk proteins. *J. Biol. Chem.* 256, 8626–8634.
- Montorzi, M., Falchuk, K. H., and Vallee, B. L. (1994) *Xenopus laevis* vitellogenin is a zinc protein. *Biochem. Biophys. Res. Commun.* 200, 1407–1413.
- Dolphin, P. J., Ansari, A. Q., Lazier, C. B., Munday, K. A., and Akhtar, M. (1971) Studies on the induction and biosynthesis of vitellogenin, an oestrogen-induced glyco-lipo-phospho-protein. *Biochem. J.* 124, 751–758.
- Wallace, R. A. (1970) Studies on amphibian yolk. IX. *Xenopus* vitellogenin. *Biochim. Biophys. Acta.* 215, 176–183.
- Tenhunen, R., Marver, H. S., and Schmid, R. (1969) Microsomal heme oxygenase: Characterization of the enzyme. *J. Biol. Chem.* 244, 6388–6394.
- Ishizawa, S., Yoshida, T., and Kikuchi, G. (1983) Induction of heme oxygenase in rat liver. Increase of the specific mRNA by treatment with various chemicals and immunological identity of the enzymes in various tissues as well as the induced enzymes. *J. Biol. Chem.* 258, 4220–4225.
- King, R. F., and Brown, S. B. (1978) The mechanism of haem catabolism. A study of haem breakdown in spleen microsomal fraction and in a model system by ^{18}O labeling and metal substitution. *Biochem. J.* 174, 103–109.

25. Opresko, L. K., and Wiley, H. S. (1987) Receptor-mediated endocytosis in *Xenopus* oocytes. I. Characterization of the vitellogenin receptor system. *J. Biol. Chem.* 262, 4109–4115.
26. Ohlendorf, D., Wrenn, R., and Banaszak, L. (1978) Three-dimensional structure of the lipovitellin–phosvitin complex from amphibian oocytes. *Nature* 272, 28–32.
27. Leonard, R., Deamer, D. W., and Armstrong, P. (1972) Amphibian yolk platelet ultrastructure visualized by freeze-etching. *J. Ultrastruct. Res.* 40, 1–24.
28. Gilbert, S. (2000) *Developmental Biology*, 6th ed., Sinauer Associates, Inc., Sunderland, MA.
29. Marinetti, G. V., and Bagnara, J. T. (1983) Yolk pigments of the Mexican leaf frog. *Science* 219, 985–987.
30. Anderson, T. A., Levitt, D. G., and Banaszak, L. J. (1998) The structural basis of lipid interactions in lipovitellin, a soluble lipoprotein. *Structure* 6, 895–909.
31. Moon, R. T., and Kimelman, D. (1998) From cortical rotation to organizer, gene expression: toward a molecular explanation of axis specification in *Xenopus*. *Bioessays* 20, 536–545.
32. Sokol, S. (1999) Wnt signaling and dorsal ventral specification in vertebrates. *Genes Dev.* 9, 405–410.
33. Cadigan, K. M., and Nusse, R. (1997) Wnt signaling: a common theme in animal development. *Genes Dev.* 11, 3286–3305.
34. DeMarais, A. A., and Moon, R. T. (1992) The armadillo homologues β catenin and plakoglobin are differentially expressed during early development of *Xenopus laevis*. *Dev. Biol.* 153, 337–346.
35. Fagotto, F., and Gumbiner, B. M. (1994) β catenin localization during *Xenopus* embryogenesis: Accumulation at tissue and somite boundaries. *Development* 120, 3667–3679.
36. Larabell, C. A., Torres, M., Miller, J. R., Rowning, B. A., Yost, C., Miller, J. R., Wu, M., Kimelman, D., and Moon, R. T. (1997) Establishment of the dorso-ventral axis in *Xenopus* embryos is presaged by early asymmetries in β catenin which are produced by *wnt* signaling. *J. Cell Biol.* 136, 1123–1136.
37. Miller, J. R., and Moon, R. T. (1996) Signal transduction through β catenin and specification of cell fate during embryogenesis. *Genes Dev.* 20, 2527–2539.
38. Behrens, J., von Kries, J., Kuhl, M., Bruhn, L., Wedlich, D., Grosschedl, R., and Birchmeier, W. (1996) Functional interaction of β catenin with the transcription factor LEF-1. *Nature* 382, 638–642.
39. Molenaar, M., van de Wetering, M., Oosterwegel, M., Peterson-Maduro, J., Godsave, S., Korinek, V., Roose, J., Destree, O., and Clevers, H. (1996) XTcf-3 transcription factor mediates β catenin-induced axis formation in *Xenopus* embryos. *Cell* 86, 391–399.
40. Dominguez, I., and Green, J. B. A. (2000) Dorsal downregulation of GSK β by a non-Wnt-like mechanism is an early molecular consequence of cortical rotation in early *Xenopus* embryos. *Development* 127, 861–868.
41. Banaszak, L., Sharrock, W., and Timmins, P. (1991) Structure and function of a lipoprotein: lipovitellin. *Annu. Rev. Biophys. Chem.* 20, 221–246.

BI020204N